

## Controllable Synthesis of Latex Particles with Multicavity Structures

Yu Huang, Jingxia Wang,\* Jinming Zhou, Liang Xu, Zhirong Li, Youzhan Zhang, Jianjun Wang, Yanlin Song,\* and Lei Jiang

Beijing National Laboratory for Molecular Sciences (BNLMS), Laboratory of New Materials, Key Laboratory of Organic Solids, Institute of Chemistry, Chinese Academy of Sciences, Beijing 100190, P. R. China

Supporting Information

## INTRODUCTION

Recently, an enormously increasing research interest has been drawn for the design and synthesis of nonspherical latex particles<sup>1–15</sup> due to their promising applications in anisotropic photonic crystals,<sup>2c,11</sup> biological sensors,<sup>7a</sup> functional coatings,<sup>3c,14,15</sup> model systems of molecules or atomic crystals,<sup>4</sup> and drug carriers.<sup>12b</sup> Generally, there are mainly three fabrication approaches<sup>5–11</sup> for nonspherical latex particles. First, the deformation of spherical latex particles is an effective way for ellipsoidal-based particles.<sup>5</sup> Over 20 types of nonspherical particles were obtained based on the stretching of spherical particles.<sup>5b</sup> Second, lithography<sup>6,7</sup> combining with the microfluidic technique is a newly developed and important means for fabricating the particles with complex shapes and sharp edge. For example, Xu et al.<sup>6b</sup> generated monodispersed latex particles (such as rods, disks, ellipsoids) with controllable size, shape, and composition from the microfluidic technique. Finally, emulsion polymerization<sup>1,8–13</sup> is a traditional and typical way for the preparation of spherical and nonspherical latex particles, which allows the control of anisotropic particles not only in shapes but also in their chemical and physical properties. Typically, Okubo et al.<sup>8</sup> synthesized anomalous polymer particles with red blood corpuscle shape. Weitz et al.<sup>9</sup> prepared triple rod, triangle, cone, diamond, and snowman-like particles in a well-controlled manner with high yield. It is highly desired to have latex particles with novel morphology and structure, which will endow the materials of special assembly structure<sup>1a</sup> and functionality.<sup>11a</sup> Herein, we demonstrate a controllable synthesis of the latex particles with various cavity structures, and the resultant film assembled from these latex particles shows interesting underwater superoleophobicity.

Currently, latex particles with cavity structures have attracted much attention since such particles may provide unique building blocks for complicated assembled structures<sup>1a</sup> and novel functional films.<sup>8a–d</sup> For example, Sacanna et al. demonstrated an intelligent lock-and-key recognition mechanism using single-cavity structured latexes as the lock and spherical latexes as the key.<sup>1a</sup> Song et al. investigated the special optical properties<sup>11a</sup> of the films assembled from latex particles with single-cavity structure. Okubo et al.<sup>8d</sup> showed a unique surfactant by using latex particles with responsive single cavity. These works were mainly focused on the synthesis and applications of latex particles with single-cavity structure,<sup>8a–d</sup> while the latex particles with multicavity structures have never been realized via emulsion polymerization due to the difficult modulation of phase separation during emulsion polymerization process, which will restrict the

development of novel assembly structures and functional films. Herein, we demonstrate a facile control of the cavity structures of the latex particles by modifying the location of phase separation just by varying the feeding way of divinylbenzene (DVB). The nonspherical latex particles with single- or multicavity and cauliflower-like structures could be successfully synthesized via emulsion polymerization. The formation of various cavity structures is mainly attributed to the single- or multilocation of PDVB at the surface of latex particles, which results in controllable phase separation on different location of latex surface and the resultant formation of latex particles with various cavity structures. Moreover, the films assembled from these nonspherical latex particles demonstrate desirable underwater superoleophobicity. This facile fabrication of the latex particles with controllable cavity structures will be of great significance for the construction of complicated assembly structures or novel functional films.

## EXPERIMENTAL SECTION

## Synthesis of the Latex Particles with Controllable Cavities.

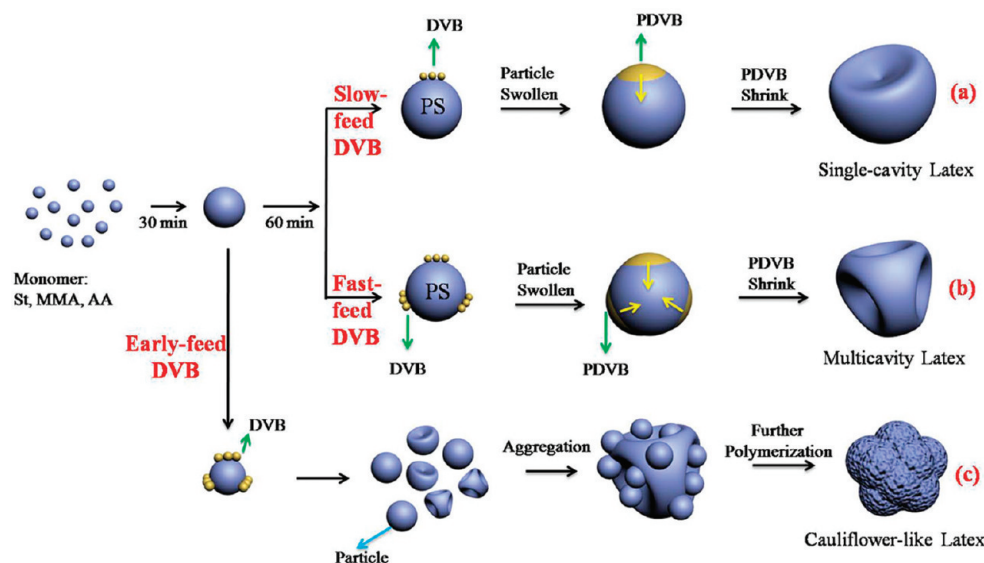
Scheme 1 demonstrates the typical experimental strategy and the possible formation procedure of the latex particles with controllable cavity structure. The latex particles were synthesized by one-step emulsion polymerization based on our previous method,<sup>11</sup> except varying the feeding modes of DVB during emulsion polymerization procedure. In details, styrene (9.5 g), methyl methacrylate (0.5 g), and acrylic acid (0.5 g) were dispersed in 50 mL of aqueous solution dissolving of emulsifier of buffer agent of  $\text{NH}_4\text{HCO}_3$  (0.5 g) and sodium dodecylbenzenesulfonate (NaDBS) (9–15 mg). After the system was heated at 70 °C, the initiator  $(\text{NH}_4)_2\text{S}_2\text{O}_8$  (APS) (0.5 g) was charged into above system, and the polymerization reaction began. Followed by the polymerization running at 70 °C for 1.5 h, the system's temperature was raised to 80 °C, and the cross-linker of DVB (0.25 g) and the initiator APS (0.25 g) were introduced into the aforementioned mixture. 2 h later, DVB (0.15 g) and APS (0.15 g) were recharged into the system. The reaction was finished after another 3 h. The resulting latex particles were used directly without any purification. In this experiment, the cavity structures of the latex particles were controlled by altering the feeding mode of DVB. The latex particles with single-cavity

Received: January 25, 2011

Revised: March 9, 2011

Published: March 25, 2011

**Scheme 1.** Possible Formation Procedure of the Latex Particles with Cavity Structures: (a) Slow-Charging Mode for Single-Cavity Latex; (b) Fast-Charging Mode for Multicavity Latex; (c) Early-Charging Mode for Cauliflower-like Latex



structure were obtained when slow-charging DVB into the system in 15 min (as shown in Scheme 1a, slow-charging mode). The latex particles with multicavity structure were obtained when fast-charging DVB into the system in 1 min (as shown in Scheme 1b, fast-charging mode). Note that the latex particles with cauliflower-like structure were obtained when charging DVB into the system earlier (as shown in Scheme 1c, early charging mode), i.e., just 0.5 h following the addition of initiator, and the feeding rate of DVB was 0.25 g in 1–15 min. The fast- or slow-charging DVB had little influence on the resultant morphology of the latex particles.

**Characterization.** Transmission electron microscope (TEM) images were obtained on a JEOL JEM-2010 transmission electron microscope operating at 200 kV. The samples were taken during the emulsion polymerization process. Conversion of monomer (weight percentage) was determined by the gravimetry. SEM images of the films were obtained using a field-emission scanning electron microscope (JSM-6700F, Japan). AFM images of the samples were characterized from Nano Scope IIIa atomic force microscopy. Contact angles (CA) were measured on an OCA20 machine (Data-Physics, Germany) at ambient temperature. Water CA was determined in air atmosphere, while oil CA was obtained by immersing the film in water and keeping downward. The oil drop of dimethylsilicone (about 2  $\mu$ L, with lower density than the water) was dropped carefully onto the surfaces. The final CA was the average value of five measurements at different positions of the same sample.<sup>15b</sup>

## RESULTS AND DISCUSSION

Scheme 1 illustrates the possible formation procedure of the latex particles with controllable cavity structures. The latex particle with single-cavity structure (in Scheme 1a) could be obtained in slow-charging mode, i.e., slow-charging DVB in 15 min after emulsion polymerization of 1.5 h. This slow addition of DVB allows the timely accumulation of DVB or PDVB in one location<sup>11</sup> at the latex surface. The as-polymerized PDVB upon

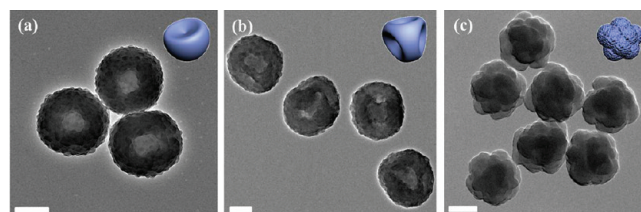


**Figure 1.** TEM images of latex particles with (a) single-cavity, (b) multicavity, and (c) cauliflower-like structure. The scale bar is 200 nm. The insert picture is the cartoon of the latex particles.

the latex surface will cause phase separation<sup>12a,16a</sup> and morphology change in one location of latex surface due to minimum Gibbs interfacial free energy, which leads to the formation of single-cavity structure at the latex surface.<sup>11</sup> In contrast, the latex particle with multicavity structure (in Scheme 1b) can be obtained in fast-charging mode, i.e., feeding DVB in 1 min. The rapid introduction of DVB makes it difficult for PDVB accumulating in one location. The multilocalized PDVB will induce the deformation of particles at multilocation of the latex surface and the resultant formation of multicavity latex structure. Alternatively, latex particles with cauliflower-like structure (in Scheme 1c) could be obtained in early-charging mode, i.e., feeding DVB into the system 30 min later of adding initiator. This process will result in multi-deformation at latex particles surface and aggregation of the latex particles at the earlier stage of polymerization.

As expected, nonspherical latex particles with various cavity structures could be synthesized by just modifying the feeding mode of DVB based in Scheme 1. Figure 1 shows TEM images of as-prepared latex particles with single- or multicavity and cauliflower-like structures. Clearly, the latex particles with single-cavity structure (also designated as mushroom-cap shaped)<sup>11</sup> in Figure 1a show the diameter of about 400 nm, with a cavity depth of about 95 nm. These latex particles are synthesized by slow-charging DVB into the emulsion polymerization system consisted of monomer of St/

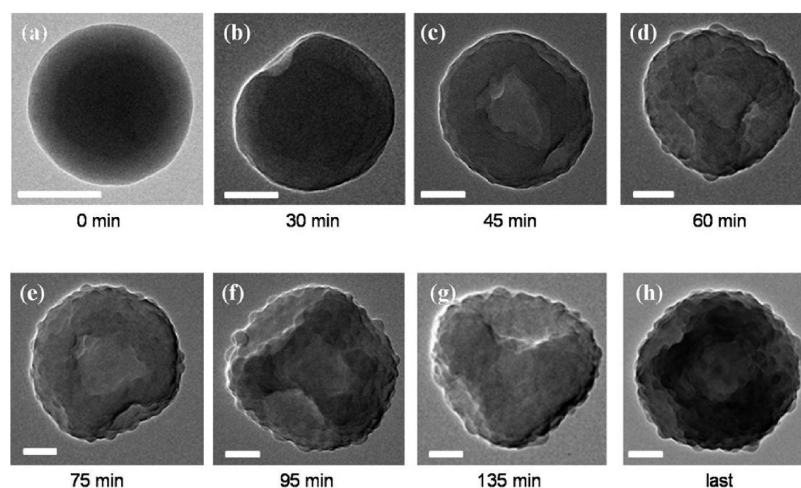


**Figure 2.** TEM images of time-dependent relationship of the latex particle synthesized from fast-charging mode; the time is determined after addition of DVB into the system. The scale bar is 100 nm.

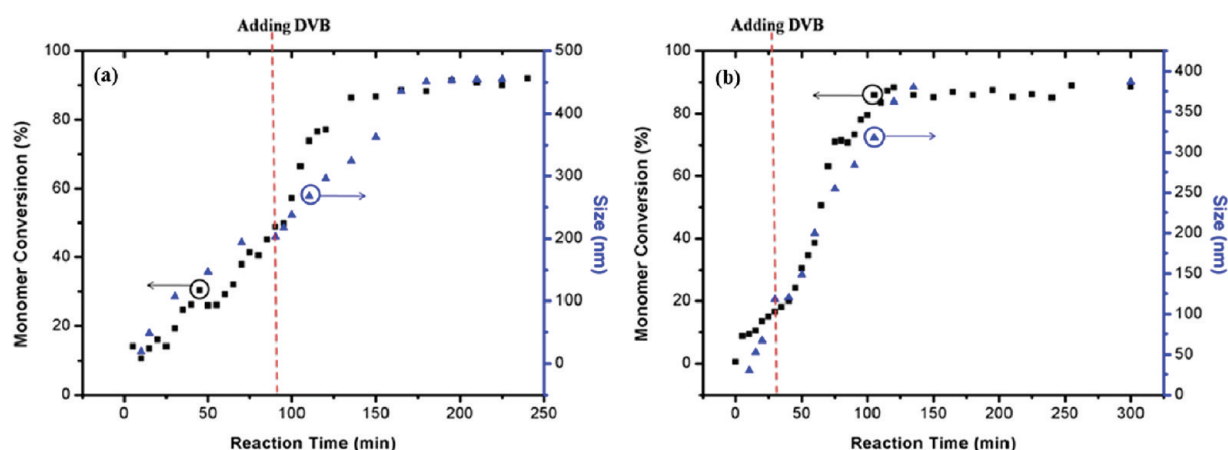


**Figure 3.** Relationship between monomer conversion (%) and reaction time (min) for emulsion polymerization of latex particles with (a) multicavity (from fast-charging mode) and (b) cauliflower-like structure (from early charging mode). The time is determined after adding of initiator.

MMA/AA after 1.5 h of initiator addition based in Scheme 1a slow-charging mode.<sup>11</sup> In comparison, the latex particles with multicavity structure (Figure 1b) are synthesized based on Scheme 1b fast-charging mode under the same conditions. There are more than three cavities on the latex surface with the latex diameter of about 450 nm, and the depth of cavities is about 50 nm, shallower than that of the single-cavity latex particle. Interestingly, cauliflower-like latex particles (with the diameter of ca. 450 nm) are synthesized by charging DVB 0.5 h after the start of emulsion polymerization (in Scheme 1c early charging mode). The latex particles with these special structures will have potential applications for the construction of the complex assembly structures.<sup>1a</sup>

To make clear the formation procedure of these latex particles, we investigate the morphology change of the latex particles and monomer conversion of the polymerization system in Figures 2, 3, and 5. Figure 2 demonstrates the morphology evolution of the latex particles with multicavity structure. The samples are obtained at different reaction time after adding DVB. At first, the latex particle shows a clear core–shell spherical structure. The darkly stained core region is rich of hydrophobic PS, which is surrounded by the lighter shell domain enrichment of hydrophilic P(MMA/AA)<sup>14c,d</sup> (Figure 2a).

Subsequently, an obvious cavity (Figure 2b) is observed at the latex surface 30 min later of charging DVB, accompanied by a rapid growth of latex diameter from 195 to 300 nm in Figure 3a. Different from the latex particles with single-cavity structure, more cavities are observed on the latex surface 45 min after adding DVB into the system (Figure 2c). The process goes with an increase of latex diameter (from 300 to 329 nm) in Figure 3a. Subsequently, little change occurs to the latex cavity's shape, but a gradual increase for latex diameter. This multicavity structure is preserved until the end of the polymerization. The formation process (in Figure 2) of the particles with multicavity structure is relevant to Scheme 1b fast-charging mode. In this process, the formation of multicavity is mainly attributed to the rapid introduction of DVB into the system, and the formed PDVB locates upon the multipositions of latex surface. The polymerized hydrophobic DVB upon latex surface will induce the phase separation<sup>12a,16a</sup> of the polymer segment at multipositions of latex surface. As a result, the hydrophobic PDVB preferably extends toward the interior of the latex particles. In the meantime, the cross-linked PDVB results in different elasticity of the polymer segment, which leads to unequilibrium shrinkage and the cavity formation on the latex particle surface.<sup>8a–c,11</sup> This



multicavity structure of latex particles is further confirmed from SEM and AFM images in Figure 4a,c. This special cavity structure will be useful for the construction of multifunctional intelligent lock–key system<sup>1a</sup> and provide unique assembly unit for novel functional films.

It is noted that the feeding time of DVB plays an important role on the resultant morphology of the latex particles as well.<sup>11a</sup> A novel latex particles with cauliflower-like structure could be obtained when early charging DVB into the emulsion system as shown in the Scheme 1c early-charging mode. Figure 5 presents TEM images of the latex particles with cauliflower-like structure taken during the formation process. Before the feeding DVB, the diameter of latex particles is 120 nm, presenting PS core PMMA/PAA shell morphology (Figure 5a). In this case, the monomer conversion of polymerization system is less than ca. 30% (Figure 3b). The residual monomer dissolves the preformed polymer segment and results in the soft and viscous latex particles, which can be proved from the chain structure in Figure 6a. Subsequently, eccentric structure of shell layer is found in Figure 5b just 10 min after the addition of DVB, which could be attributed that the soft and viscous latex particle favors the random location of PDVB on

the latex surface. The presence of PDVB on latex surface will induce the phase separation<sup>12a</sup> of polymer segment and the deformation of the latex particles. As a result, a large cavity (Figure 5c) occurs to the latex particle in 20 min after adding DVB, accompanied by an increase in the latex diameter. This cavity formation of the latex particle is earlier than that in Figure 2b. Multicavity structure (Figure 5d) could be further observed in 30 min after the addition of DVB, with an obvious growth of latex diameter from 148 to 200 nm in Figure 3b. This evident increase of latex diameter may be aroused from the coalescence among latex particles. Surprisingly, a great viscosity increase lasting for 10 min is found for the emulsion polymerization after 20 min after the addition of DVB, which could be confirmed by the difficult sampling. When the viscosity increases, the sample cannot be directly taken out from the flask by sucking. This unexpected viscosity growth may be arisen from the solvency of the residual St to the polymer segment containing rigid PDVB, which is favorable for the random location of PDVB on the latex surface. This multilocation of PDVB results in phase separation accompanied by the polymerization of the residual monomer and the regrowth of the latex diameter due to particles' aggregation, which contributes to the formation of more cavities in the latex surface. This procedure persists to 75 min (Figure 5g) after adding DVB. The combination of phase separation and latex aggregation will rationalize the cavity structure, as contributes to the resultant formation of latex particle with cauliflower-like structure (Figure 5h). The cauliflower structure of the latex surface can be observed from SEM and AFM images in Figure 4b, d as well. The uneven surface of cauliflower-like structure endows the hierarchical structure to latex particles, which will contribute to the special functionality for the resultant film.

Interestingly, a typical aggregation of different latex particles is observed (Figure 6b–d) during the emulsion polymerization process; i.e., small particles with diameter of about 120 nm aggregate together to form larger particles with multicavity structure. This process results in a growth of the latex particles and the formation of different latex morphology. That is, the introduction of DVB causes the cavity structure of latex surface, while latex aggregation leads to an increase of latex diameter and the formation of latex with cauliflower-like structure.<sup>16b</sup> The formation process of the particles with cauliflower-like structure is corresponding to Scheme 1c early charging mode. The

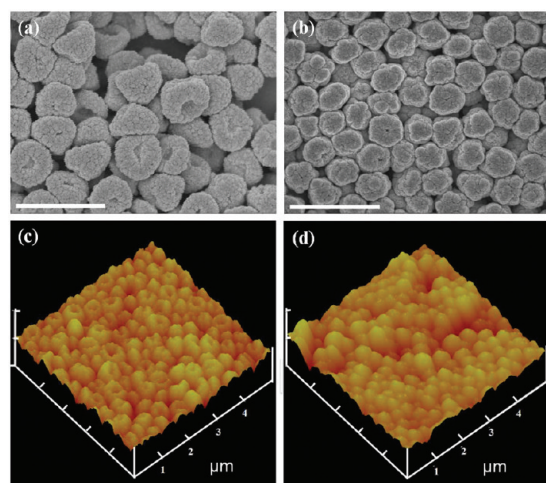


**Figure 4.** SEM and AFM images of films assembled from the latex with (a, c) multicavity and (b, d) cauliflower-like structure. The scale bar is 1  $\mu\text{m}$ .

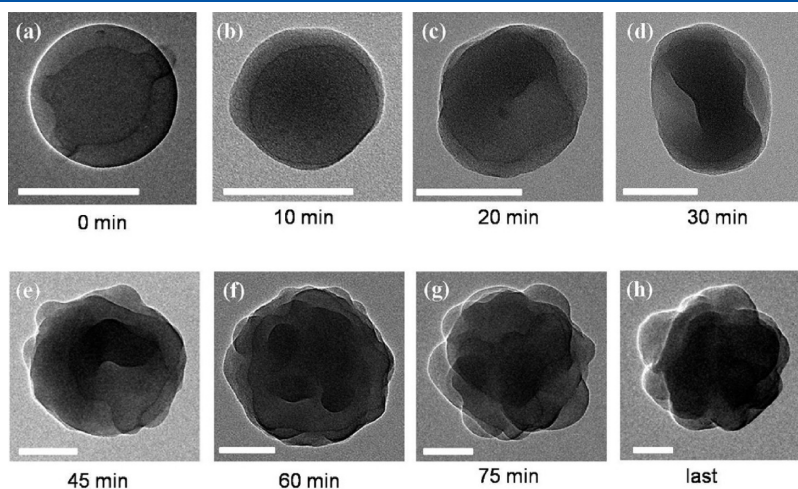


**Figure 5.** TEM images of time-dependent relationship of the latex particle synthesized from early charging mode; the time is determined after addition of DVB into the system. The scale bar is 100 nm.

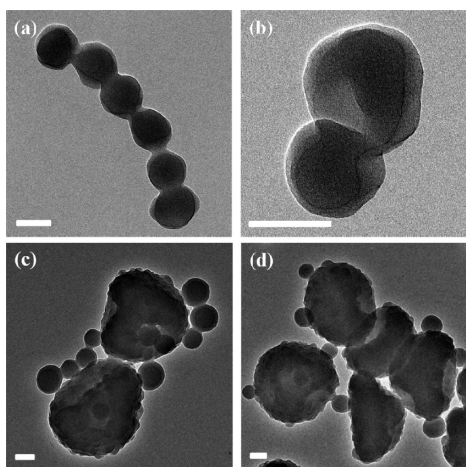


**Figure 6.** TEM image of the latex particles (a) with chain structure due to the viscous latex surface and (b–d) typical aggregation of the latex particles during polymerization. The scale bar is 100 nm.

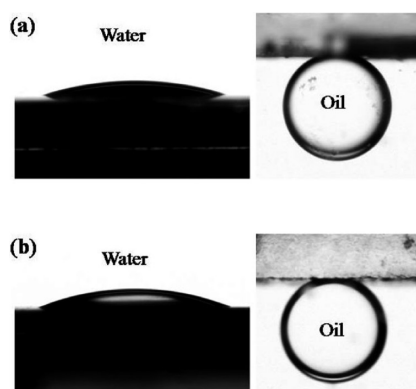


**Figure 7.** Shape of the water/oil on the film assembled from (a) multicavity and (b) cauliflower-like structure. The water contact angle was obtained in air, while oil contact angle was obtained when put the film into water.

monodispersity of as-prepared nonspherical latex particles is very important. For the multicavity structured latex particles, the monodispersity of the particles refers not only to the dimension of the particles but also to the cavity location and depth. The dimension, cavity structure, and depth of particles can be obtained from TEM and AFM. In our case, the dimension of particles are also determined by dynamic light scattering (Figure S2).

Additionally, the special wettability of films assembled from as-prepared nonspherical latex particle is demonstrated in Figure 7. The water CAs of films from the particles of multicavity and cauliflower-like structures are  $16.7 \pm 1.3^\circ$  and  $19.2 \pm 1.2^\circ$ , respectively, demonstrating the high hydrophilicity in air. When put the films into water, the oil CAs of the films are  $160.5 \pm 2.1^\circ$  and  $159.5 \pm 1.3^\circ$ , respectively, indicating the underwater superoleophobicity.<sup>15b</sup> The high hydrophilicity mainly resulted from the hydrophilic PAA shell of latex surface, while the water adsorbed layer of hydrophilic shell leads to the underwater superoleophobicity. This special wettability could be ascribed to the combination of both the surface chemical composition and their special rough structure, which will be of significance for the potential use of functional coating.<sup>14,15</sup>

## CONCLUSIONS

In conclusion, the latex particles with single-cavity, multicavity, and cauliflower-like structures could be controllably synthesized by modifying the feeding mode of DVB during emulsion polymerization procedure. The different feeding modes of DVB affect the location of PDVB on the latex surface based on the amount of the residual monomer and the system's viscosity, which leads to the formation of the latex particles with different cavity structures. The synthesis of these latex particles with controllable cavity structure provides not only novel building blocks for the construction of complex colloidal architecture but also a new insight for the fabrication of colloidal films with desirable functionalities.

## ASSOCIATED CONTENT

**S Supporting Information.** DLS data of as-prepared latex particles; TEM and AFM images of the films assembled from the nonspherical latex particles. This material is available free of charge via the Internet at <http://pubs.acs.org>.

## AUTHOR INFORMATION

### Corresponding Author

\*E-mail: wangzhang@iccas.ac.cn (J.W.), ylsong@iccas.ac.cn (Y.S.).

## ACKNOWLEDGMENT

This work is supported by the NSFC (Grants 50973117, 21074139, 20904061, 50625312, U0634004, and 20721061) and the 973 program (2007CB936403 and 2009CB930404, 2011CB932303, 2011CB808400). The authors thank the beneficial discussions from Prof. Chengyou Kan and Prof. Zhaoxia Guo at Tsinghua University.

## REFERENCES

- (1) (a) Sacanna, S.; Irvine, W. T. M.; Chaikin, P. M.; Pine, D. J. *Nature* **2010**, *464*, 575–578. (b) Yang, S. M.; Kim, S. H.; Lim, J. M.; Yi, G. R. *J. Mater. Chem.* **2008**, *18*, 2177–2190.
- (2) (a) Im, S. H.; Jeong, U.; Xia, Y. N. *Nature Mater.* **2005**, *4*, 671–675. (b) Ge, J.; Hu, Y.; Zhang, T.; Yin, Y. *J. Am. Chem. Soc.* **2007**, *129*, 8974–8975. (c) Ding, T.; Song, K.; Clays, K. *Adv. Mater.* **2009**, *21*, 1936–1940. (d) Li, Y. F.; Zhang, J. H.; Yang, B. *Nano Today* **2010**, *5*, 117–127.
- (3) (a) Feyen, M.; Weidenthaler, C.; Schuth, F.; Lu, A. H. *J. Am. Chem. Soc.* **2010**, *132*, 6791–6799. (b) Jeon, S. J.; Yi, G. R.; Yang, S. M. *Adv. Mater.* **2008**, *20*, 4103–4108. (c) Kim, S. H.; Lee, S. Y.; Yang, S. M. *Angew. Chem., Int. Ed.* **2010**, *49*, 2535–2638.
- (4) (a) Yethiraj, A.; van Blaaderen, A. *Nature* **2003**, *421*, 513–517. (b) Kegel, W. K.; van Blaaderen, A. *Science* **2000**, *287*, 290–293.
- (5) (a) Ho, C. C.; Keller, A.; Odell, J. A.; Ottewill, R. H. *Colloid Polym. Sci.* **1993**, *271*, 469–479. (b) Champion, J. A.; Katare, Y. K.; Mitragotri, S. *Proc. Natl. Acad. Sci. U.S.A.* **2007**, *104*, 11901–11904. (c) Jiang, P.; Bertone, J. F.; Colvin, V. L. *Science* **2001**, *291*, 453–457.
- (6) (a) Dendukuri, D.; Pregibon, D. C.; Collins, J.; Hatton, T. A.; Doyle, P. S. *Nature Mater.* **2006**, *5*, 365–369. (b) Xu, S. Q.; Nie, Z. H.; Seo, M.; Lewis, P.; Kumacheva, E.; Stone, H. A.; Garstecki, P.; Weibel, D. B.; Gitlin, I.; Whitesides, G. M. *Angew. Chem., Int. Ed.* **2005**, *44*, 724–728.
- (7) (a) Seiffert, S.; Thiele, J.; Abate, A. R.; Weitz, D. A. *J. Am. Chem. Soc.* **2010**, *132*, 6606–6609. (b) Kim, S. H.; Jeon, S. J.; Jeong, W. C.; Park, H. S.; Yang, S. M. *Adv. Mater.* **2008**, *20*, 4129–4134.
- (8) (a) Okubo, M.; Minami, H. *Colloid Polym. Sci.* **1997**, *275*, 992–997. (b) Okubo, M.; Minami, H. *Macromol. Symp.* **2000**, *155*, 1–10.

150, 201–210. (c) Tanaka, T.; Okayama, M.; Kitayama, Y.; Kagawa, Y.; Okubo, M. *Langmuir* **2010**, *26*, 7843–7847. (d) Tanaka, T.; Okayama, M.; Minami, H.; Okubo, M. *Langmuir* **2010**, *26*, 11732–11736. (e) Tanaka, T.; Saito, N.; Okubo, M. *Macromolecules* **2009**, *42*, 7423–7429.

(9) (a) Kim, J. W.; Larsen, R. J.; Weitz, D. A. *J. Am. Chem. Soc.* **2006**, *128*, 14374–14377. (b) Kim, J. W.; Larsen, R. J.; Weitz, D. A. *Adv. Mater.* **2007**, *19*, 2005–2009.

(10) (a) Park, J. G.; Forster, J. D.; Dufresne, E. R. *J. Am. Chem. Soc.* **2010**, *132*, 5960–5961. (b) Yu, H. K.; Mao, Z. W.; Wang, D. Y. *J. Am. Chem. Soc.* **2009**, *131*, 6366–6367. (c) Mock, E. B.; Bruyn, H. D.; Hawkett, B. S.; Gilbert, R. G.; Zukoski, C. F. *Langmuir* **2006**, *22*, 4037–4043.

(11) (a) Xu, L.; Li, H.; Jiang, X.; Wang, J. X.; Li, L.; Song, Y. L.; Jiang, L. *Macromol. Rapid Commun.* **2010**, *31*, 1422–1426. (b) Lv, H.; Lin, Q.; Yang, B. *Langmuir* **2008**, *24*, 13736–13738.

(12) (a) Hao, D. X.; Gong, F. L.; Hu, G. H.; Lei, J. D.; Ma, G. H.; Su, Z. G. *Polymer* **2009**, *50*, 3188–3195. (b) Wei, W.; Ma, G. H.; Hu, G.; Yu, D.; Mcleish, T.; Su, Z. G.; Shen, Z. Y. *J. Am. Chem. Soc.* **2008**, *130*, 15808–15810. (c) Medina-Castillo, A. L.; Fernandez-Sanchez, J. F.; Segura-Carretero, A.; Fernandez-Gutierrez, A. *Macromolecules* **2010**, *43*, 5804–5813. (d) Voorn, D. J.; Ming, W.; van Herk, A. M. *Macromolecules* **2006**, *39*, 4654–4656.

(13) (a) Cao, Z.; Ziener, U.; Landfester, K. *Macromolecules* **2010**, *43*, 6353–6360. (b) Zhang, J.; Yang, J.; Wu, Q.; Wu, M.; Liu, N.; J., Z.; Wang, Y. *Macromolecules* **2010**, *43*, 1188–1190. (c) Herrera, V.; Palmillas, Z.; Pirri, R.; Reyes, Y.; Leiza, J. R.; Asua, J. M. *Macromolecules* **2010**, *43*, 1356–1363.

(14) (a) Zhu, D. F.; Li, X. A.; Zhang, G.; Zhang, X.; Zhang, X. M.; Wang, T. Q.; Yang, B. *Langmuir* **2010**, *26*, 14276–14283. (b) Wang, T. Q.; Li, X. A.; Zhang, J. H.; Wang, X. Z.; Zhang, X. M.; Zhang, X.; Zhang, D. F.; Hao, Y. D.; Ren, Z. Y.; Yang, B. *Langmuir* **2010**, *26*, 13715–13721. (c) Wang, J. X.; Wen, Y. Q.; Feng, X. J.; Song, Y. L.; Jiang, L. *Macromol. Rapid Commun.* **2006**, *27*, 188–192. (d) Wang, J. X.; Wen, Y. Q.; Ge, H. L.; Sun, Z. W.; Zheng, Y. M.; Song, Y. L.; Jiang, L. *Macromol. Chem. Phys.* **2006**, *207*, 596–604.

(15) (a) Du, C. G.; Zhang, Y. Z.; Zhao, T. Y.; Wang, J. X.; Song, Y. L.; Jiang, L. *J. Nanosci. Nanotechnol.* **2010**, *10*, 7766–7769. (b) Liu, M. J.; Wang, S. T.; Wei, Z. X.; Song, Y. L.; Jiang, L. *Adv. Mater.* **2009**, *21*, 665–668. (c) Wang, J. X.; Zhang, Y. Z.; Zhao, T. Y.; Song, Y. L.; Jiang, L. *Sci. China, Ser. B: Chem.* **2010**, *53* (2), 318–326. (d) Wang, J. X.; Zhang, Y. Z.; Wang, S. T.; Song, Y. L.; Jiang, L. *Acc. Chem. Res.* **2011** ar-2010-001236.

(16) (a) Okay, O. *Prog. Polym. Sci.* **2000**, *25* (6), 711–779. (b) Mendizabal, E.; Flores, J.; Puig, J. E.; Lopez-serrano, F.; Alvarez J. *Eur. Polym. J.* **1998**, *34* (3), 411–420.

(17) (a) *Dynamic Light Scattering: Applications of Photon Correlation Spectroscopy*, 1st ed.; Pecora, R., Ed.; Plenum Press: New York, 1985. (b) *Light Scattering by Nonspherical Particles: Theory, Measurements and Applications*, 1st ed.; Mishchenko, M. I.; Hovenier, J. W., Travis, L. D., Eds.; Academic Press: San Diego, CA, 2000; p 30. (c) Pencer, J.; Hallett, F. R. *Langmuir* **2003**, *19*, 7488–7497.